Journal of the Ceramic Society of Japan 121 [6] 512-515 2013 Paper

Influence of density of state of ferromagnetic filter layer in charge injection properties of Si metal–insulator–semiconductor capacitor with a magneto-electric gate insulator

Takeshi YOKOTA,† Shotaro MURATA and Manabu GOMI

Materials Science and Engineering, Nagoya Institute of Technology, Gokiso-cho, Showa-ku, Nagoya 466–8555, Japan

We investigated the detailed charge injection properties of a metal (Pt)/insulator (Cr_2O_3)/floating gate layer (Cr_2O_{3-x})/magnetic filtering layer/tunnel layer (CeO_2)/semiconductor (Si) capacitor. This capacitor shows charge injection type capacitance–voltage (C–V) properties with a hysteresis window. The hysteresis window width (HWW) can be controlled by an external electric or magnetic field. Changes in the HWW are determined by the combined spin density of state of a spin filter layer and a floating gate. Our results indicate that this capacitor may be able to electromagnetically store multiple charges.

Key-words : Magneto-electric effect, Dielectric properties, Capacitance measurement, MIS devices

[Received February 18, 2013; Accepted April 18, 2013]

1. Introduction

Magnetoelectric (ME) devices employing ME materials have become attractive as a new generation of non-volatile data storage devices, because their magnetic or ferroelectric properties can be controlled by an external electric or magnetic field.[1)–4)] Although many researchers are investigating ME materials, there are only a few reports of electric devices using the ME feature.[5)–7)] Previously, we proposed the possibility of ME capacitors (MECs) consisting of Pt/Cr_2O_3 (ME material:gate insulator)/Cr_2O_{3-x} (floating gate: F.G.)/Fe (magnetic filtering layer: MFL)/CeO_2/Si.[8)] By the application of electric and magnetic fields at the same time, charges injected into the F.G. were modulated depending on the magnetic field. Although the injected carrier was controlled by an external electric and magnetic field, the injection mechanism was still not clear. In the present study, we examined the relationships between magnetic properties and the charge injection process and investigated the role of a magnetic filtering layer by using a sample with different magnetic filtering layers.

2. Experiment

MECs were prepared using the 3-guns radio-frequency magnetron sputtering method. Cr_2O_3 and CeO_2 sintered ceramics were used as the target. The base pressure before introducing the sputtering gas was 3.0×10^{-4} Pa, and the gas pressure during deposition was 8.0×10^{-1} Pa. First, a 5-nm-thick CeO_2 tunnel layer was deposited on an n-type Si(111) substrate that had been cleaned using improved Radio Corporation of America methods. Next, we deposited various MFLs, which were Fe, $Fe_{50}Cr_{50}$, $Ni_{82}Fe_{18}$, and Fe_3O_4 layers with a thickness of 0.25 nm, respectively, using only Ar as the sputtering gas. The F.G., which was a 1-nm-thick Cr_2O_{3-x} layer, was then deposited using only Ar as the sputtering gas. Finally, a 45-nm-thick Cr_2O_3 layer was deposited. The magnetic properties of the sample were measured using a superconducting quantum interface device (SQUID). The structural analysis of the films was performed using an X-ray diffractometer (XRD) utilizing Cu Kα radiation and reflected high-energy electron diffraction (RHEED). The surface morphology was measured using an atomic force microscope (AFM). The leakage current was measured using a picoammeter (Keithley-6487), while capacitance was measured using an inductance, capacitance, resistance (LCR) meter (Agilent, E6480A). Pt and Au were used as the top and bottom electrodes, respectively. To avoid a measurement deviation, we performed electric property measurements with about 40 electrodes constructed on the sample.

3. Results and discussion

Figure 1 shows capacitance–voltage (C–V) characteristics of the sample with/without an external magnetic field having various MFLs. The inset shows a schematic illustration of the measurement. Every C–V curve exhibits hysteresis with a clockwise trace, indicating that electrons have been injected into the Cr_2O_{3-x} layer.[9)] When a 5 mT magnetic field is applied to the sample surface, only the capacitance trace from the carrier injection process is shifted to the negative voltage direction for Fe (at around 0–1.5 V) and $Fe_{50}Cr_{50}$ (at around 0–1 V), and to the positive voltage direction for $Ni_{82}Fe_{18}$ (at around 0–1 V). **Figure 2** shows the magnetic field dependence of the hysteresis window width (HWW) of those samples. The HWW of the sample having a Fe or a $Ni_{82}Fe_{18}$ layer increased or decreased with the increase of an external magnetic field, respectively. In the case of the sample having $Fe_{50}Cr_{50}$, the HWW barely showed negative changes until 2 mT. Above 2 mT, the changes increased with the increase of an external magnetic field.

To investigate the charge injection properties, we measured magnetoresistance (MR) for various magnetic fields. The measurement direction of the MR was the same as that for the C–V measurement, because we assumed that a current indicated a carrier injection process into the Cr_2O_{3-x} floating layer. It is also important to take the measurement voltages into account, because carrier injection occurs above the flat-band voltage.[10)] According

† Corresponding author: T. Yokota; E-mail: yokota.takeshi@nitech.ac.jp

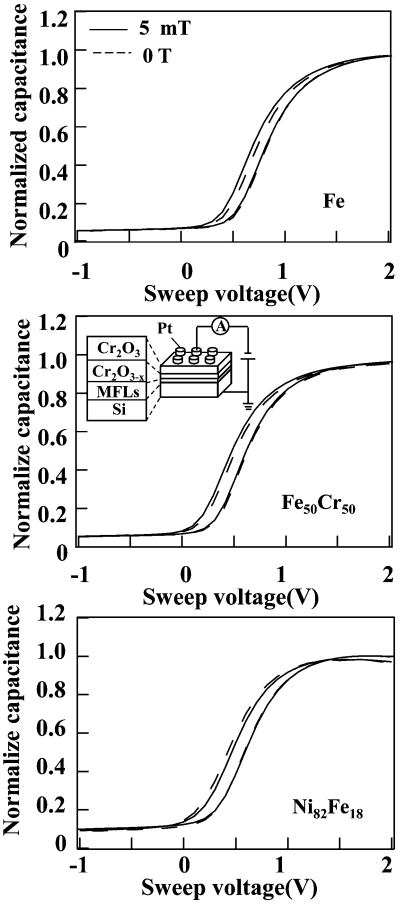

Fig. 1. C–V characteristics of the Cr_2O_3/Cr_2O_{3-x}/MFL/CeO_2/Si capacitor with various magnetic filtering layers. The samples are measured with (5 mT)/without the external magnetic field. Inset shows a schematic illustration of the measurement.

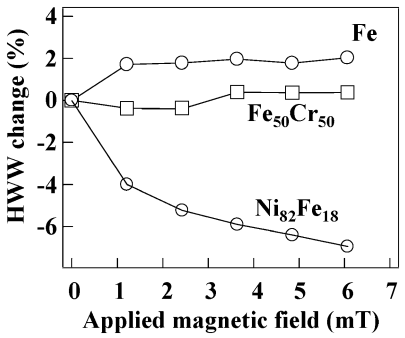

Fig. 2. Changes in the HWW of the sample with various MFLs against an external magnetic field.

to the depletion layer approximation, the experimental flat-band voltage of this capacitor is about 0.1 V.[11] We decided to use the relatively high voltage of 0.15 V for measurement, because every C–V curve showed a slightly flat band-shift. **Figure 3** shows the results of MR measurement. The resistance of the sample with a Fe and $Fe_{50}Cr_{50}$ layer increased below 1 mT and then decreased with the increase of the magnetic field. On the other hand, the sample with a $Ni_{82}Fe_{18}$ layer increased with the increase of the magnetic field. These MR results show the same tendency as that of the results of HWW changes. Since the increasing/decreasing of resistance by the application of a magnetic field, i.e., the decrease/increase of current, means that the electron

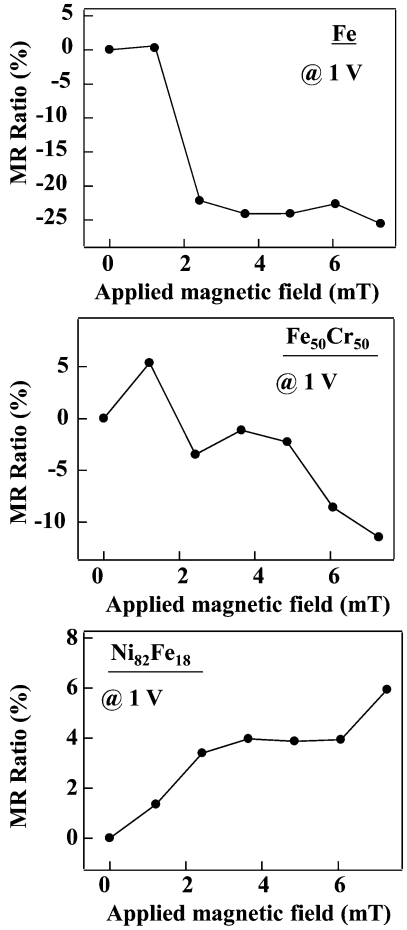

Fig. 3. MR of the Cr_2O_3/Cr_2O_{3-x}/MFL/CeO_2/Si capacitor with various magnetic filtering layers measured at 1 V.

charge in the capacitor increases, these tendencies are reasonable. This charge injection mechanism also seems to be related to the magnetization state of the MFL and F.G., both of which are ferromagnetic. Generally, MR could be described with the theory of Drude-Lorentz.[12] Since the effect was considered by treating the electric current density and magnetic field as vector quantities, the galvanomegnetic effect on the relationship between them can be expressed by the following equation:

$$E = \sigma(1 - GB^2 \sin\theta)j$$

(E: electric field, σ: conductivity, G: constant, B: magnetic field, j: current)

Since θ shows the angle between the vector of magnetic flux density and electric current density, anisotropy is observed according to the direction of magnetization, even if the materials are isotropic. Furthermore, in the case of ferromagnetism, magnetic flux density, B, can be explained as the sum of the external magnetic flux density, B_0, and internal magnetic field, M. According to this equation, negative MR originated from decreases in elastic electron scatterings due to aligning of the magnetic moment. If the F.G. layer wasn't a magnetic layer, the amount of the injected charges increased, depending on the degree of the magnetic moment alignment of the MFL layer. Then, the total amount of injectable charges corresponded to the number of injection sites in the F.G. The HWW changes at a low magnetic field in the sample with Fe and $Fe_{50}Cr_{50}$ can also be explained by this mechanism. This does not explain the behavior

of $Ni_{82}Fe_{18}$; however, we considered one possible solution. We focused on the spin density of state (DOS) of each layer, because it is a similar structure to the magnetic stack structure showing giant MR (GMR).[13] The GMR was composed of alternating ferromagnetic and non-magnetic conductive layers. The resistance changes depended on whether the magnetization of adjacent ferromagnetic layers was in parallel or antiparallel, which corresponds to the DOS of each layer. In the case of our sample, the majority spin DOS of Fe, $Fe_{50}Cr_{50}$, and Cr_2O_{3-x} is up.[14)–16)] Although to our knowledge the energy bands of $Ni_{82}Fe_{18}$ have not been mapped yet, extensive investigation of Ni and Ni–Fe compounds has occurred. For example, Petrovykh et al. discussed the energy band structure of $Ni_{82}Fe_{18}$ and found that the spin band of $Ni_{82}Fe_{18}$ is relatively dominated by a Ni d band compared with the Fe d band.[17)] The majority spin DOS of Ni is down.[18)] The majority spin state of Ni_3Fe is also down. Therefore, $Ni_{82}Fe_{18}$ should have majority down-spin DOS. Based on this assumption, the mismatching of the majority spin DOS is likely responsible for the charge injection behavior. If the sign of the majority spin state matches the MFG layer to the F.G. layer, the carriers are easily injected into the F.G. layer. If it is the opposite, the carriers cannot be injected.

To test our hypothesis, we prepared a sample with Fe_3O_4 as a MFL, which is a half-metallic state predicted by the band-structure calculations, with nearly 100% spin polarization, and a down-spin majority spin state.[19),20)] By using this spin-polarized spin filter, we expected to clarify the role of a Cr_2O_{3-x} F.G. Before measuring the injection properties, we measured the magnetization of this sample to check the magnetic properties at room temperature. The sample showed a saturation magnetization of 400 emu/cc. The saturation magnetization is about 85% of the reported bulk value of 471 emu/cc.[21),22)] Although we didn't check the half-metallic feature of our sample, we expected that most of the spins were polarized from this result. **Figure 4**(a) shows the C–V characteristics of the sample with/without an external magnetic field with a Fe_3O_4 MFL. In this case, we used a relatively high measurement magnetic field compared with the other samples, as the coercive force of our Fe_3O_4 was about 30 mT. With the application of a magnetic field, the HWW of the C–V curve decreased. In particular, the ejection process, which is indicated by the arrow in Fig. 4(a), shifted to negative voltage when compared with the injection process. This means some of the charges are magnetically scattered by the spin filtering effect during the injection process, reducing the amount of stored charge based on the mechanism described above. The total changing ratio is much larger than that of the other samples, presumably due to the high degree of spin polarization originating from the half-metallic feature of Fe_3O_4. Figure 4(b) shows an applied magnetic field dependence of HWW. In the low magnetic field, the HWW increased and then decreased. In the initial stage the spins in the MFL are not totally aligned by the external magnetic field. Therefore, minority up spins can be injected by the applied electric field, just as occurs with a common semiconductor capacitor. Above 30 mT, the HWW value, even if it is different depending on the magnetic field, is gradually decreased. This HWW change difference can be explained by a mechanism similar to that described above. Although the majority spin DOS of Cr_2O_{3-x} is up, a minority down spin state remains.[16)] In addition to that, Cr_2O_{3-x} is a ME material, and its ME state should be changed by the application of an electric and magnetic field.[20)] Therefore, the minority down spin state of Cr_2O_{3-x} can be matched to the down spin state of half-metallic Fe_3O_4 by the application of both a magnetic and an electric field. When this matching occurs, charges could be stored in the F.G. Since this matching depends on the electric and magnetic field, the HWW charge differences can be observed. Even though the amount of injected charges is increasing and decreasing, the total charge in the capacitor decreases within the measurement voltage. Therefore, the amount of injectable charges is dominated by the sign of the filtering layer. Although we still need to optimize the electric and magnetic field to control the amount of injected charges and stored charges, this result may give rise to an electro-magnetically charged capacitor.

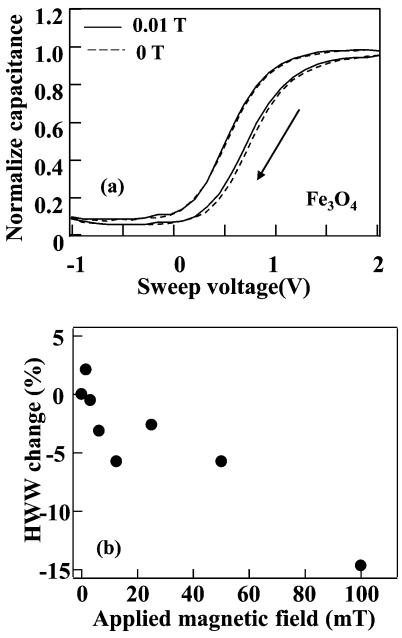

Fig. 4. (a) C–V characteristics and (b) MR of the $Cr_2O_3/Cr_2O_{3-x}/Fe_3O_4/CeO_2/Si$ capacitor. The C–V characteristics are measured with (0.01 T)/without the external magnetic field.

4. Conclusion

We prepared a ME field effect capacitor and investigated the relationships between the charge injection properties and the magnetic filtering layers. The charge injection properties vary depending on the combination of the filtering layer and the F.G. MR measurement revealed that the amount of charge injection corresponding to the amount of the carrier affected the external magnetic field. The carrier is influenced by the combination of the spin DOS of the filter layer and the F.G. In other words, the combination of an up/up spin DOS increases the injected charges, and the opposite decreases the charges. A half-metal filtering layer is effective for changing the amount of injected charges by an external magnetic field. These results indicate that this metal–insulator–semiconductor capacitor has two kinds of charge that are electrically and magnetically controlled.

Acknowledgments This work was supported in part by a Grant-in-Aid for Young Scientists (A) (23686094) from the Japan Society for the Promotion of Science (JSPS) and the JSPS International Training Program (ITP), "Young Scientist-Training Program for World Ceramics Network", and in part by a grant from the Institute of Ceramics Research and Education, NITECH.

References

1) N. Hur, S. Park, P. A. Sharma, J. S. Ahn, S. Guha and S.-W. Cheong, *Nature*, 429, 392–395 (2004).

2) T. Lottermoser, T. Lonkai, U. Amann, D. Hohlwein, J. Ihringer and M. Fiebig, *Nature*, 430, 541–544 (2004).
3) J. Wang, J. B. Neaton, H. Zheng, V. Nagarajan, S. B. Ogale, B. Liu, D. Viehland, V. Vaithyanathan, D. G. Schlom, U. V. Waghmare, N. A. Spaldin, K. M. Rabe, M. Wuttig and R. Ramesh, *Science*, 299, 1719–1722 (2003).
4) Y. K. Yun, M. Noda and M. Okuyama, *Appl. Phys. Lett.*, 83, 3981–3983 (2003).
5) J. Zhai, Z. Xing, S. Dong, J. Li and D. Viehland, *Appl. Phys. Lett.*, 88, 062510 (2006).
6) N. X. Sun and G. Srinivasan, *SPIN*, 02, 1240004 (2012).
7) G. Sreenivasulu, U. Laletin, W. M. Petrov, V. V. Petrov and G. Srinivasan, *Appl. Phys. Lett.*, 100, 173506 (2012).
8) T. Yokota, S. Murata, S. Kito and M. Gomi, *J. App. Phys.*, 105, 07D905 (2009).
9) T. Yokota, S. Murata, T. Kuribayashi and M. Gomi, *J. Ceram. Soc. Jpn.*, 116, 1204–1207 (2008).
10) T. Nakagawa and H. Fujisada, Solid-State and Ele. Dev., IEE Proc., Vol. 131, Pt. 1, No. 2 (1984) pp. 51–55.
11) S. M. Sze, "Semiconductor Physics", 2nd edition, Wiley-Interscience, New York (1981) pp. 374–391.
12) G. Giuliani, *Europhys. Lett.*, 81, 60002–60008 (2008).
13) M. N. Baibich, J. M. Broto, A. Fert, F. Nguyen Van Dau, P. Etienne, G. Creuzet, A. Friederich and J. Chazelas, *Phys. Rev. Lett.*, 61, 2472–2475 (1988).
14) S. Serdouk, R. Hayn and J.-L. Autran, *J. Appl. Phys.*, 102, 113707 (2007).
15) P. Olsso, I. A. Abrikosov and J. Wallenius, *Phys. Rev. B*, 73, 104416 (2006).
16) P. S. Robbert and H. Geisler, *J. Vac. Sci. Technol., A*, 16, 990–995 (1998).
17) D. Y. Petrovykh, K. N. Altmann, H. Höchst, M. Laubscher, S. Maat, G. J. Mankey and F. J. Himpsel, *Appl. Phys. Lett.*, 73, 3459–3461 (1998).
18) A. Yanase and N. Hamada, *J. Phys. Soc. Jpn.*, 68, 1607–1613 (1999).
19) Y. S. Dedkov, U. Rüdiger and G. Güntherodt, *Phys. Rev. B*, 65, 064417 (2002).
20) Ch. Binek, A. Hochstrat, X. Chen, P. Borisov, W. Kleemann and B. Doudin, *J. Appl. Phys.*, 97, 10C514 (2005).
21) L. R. Bickford, Jr., *Phys. Rev.*, 78, 449–457 (1950).
22) S. Kale, S. M. Bhagat, S. E. Lofland, T. Scabarozi, S. B. Ogale, A. Orozco, S. R. Shinde, T. Venkatesan, B. Hannoyer, B. Mercey and W. Prellier, *Phys. Rev. B*, 64, 205413 (2001).